TESTING THE MEMORY-RETRIEVAL MODEL OF GRID CELLS

ARE PHYSICAL SPACE AND PERCEPTUAL COLOR SPACE EFFICIENTLY REPRESENTED USING A COMMON CONSOLIDATION ALGORITHM?

An Honors Thesis

Presented by

Nicholas Blauch

Completion Date:
June 2017

Approved By:

_____

David E. Huber, Chair. Dept. of Psychological and Brain Sciences.

_____

Rosie A. Cowell, Committee Member. Dept. of Psychological and Brain Sciences

ABSTRACT

Title: TESTING THE MEMORY RETRIEVAL MODEL OF GRID CELLS: ARE PHYSICAL SPACE AND COLOR SPACE EFFICIENTLY REPRESENTED USING A COMMON CONSOLIDATION ALGORITHM?
Author: Nicholas Blauch
Thesis/Project Type: Independent Honors Thesis
Approved By: David E. Huber, Chair. Dept. of Psychological and Brain Sciences.
Approved By: Rosie A. Cowell, Committee Member. Dept. of Psychological and Brain Sciences

"Grid cells" in the medial entorhinal cortex (MEC) are proposed as the GPS coordinates in the computation of self-location downstream in the hippocampus (HC), where individual "place cells" fire in a specific place in an environment. To account for findings contradictory to this model, Huber & Solstad have proposed an alternative Memory-Retrieval Model of grid cells (submitted), which frames the grid response as the result of feedback from efficiently consolidated hippocampal episodes. The optimal consolidation algorithm is proposed as a universal consolidation algorithm in a representational hierarchical view of the brain, where different regions perform fundamentally similar operations on different types of information. Thus, we suggest that navigation in non-spatial perceptual and conceptual spaces will yield a grid-like signal in the cortical areas dedicated to processing these stimulus dimensions. To evaluate this proposal, we design a human functional magnetic resonance imaging (fMRI) study to test for the presence of a grid-like signal in visual cortex in response to "navigation" in a perceptual color space. Here, I analyze behavioral color similarity ratings in order to compute an individual's 2D perceptual color space, and analyze BOLD similarity patterns in order to compute a 2D cortical color space, both of which can be used to calibrate analyses of the grid-like pattern. While the behavioral experiment yields reasonable perceptual color spaces, we determine that more neuroimaging data needs to be collected both to compute cortical color spaces, and to test for grid-like responses to navigation in color space.

ABSTRACT

Title: TESTING THE MEMORY RETRIEVAL MODEL OF GRID CELLS: ARE PHYSICAL SPACE AND COLOR SPACE EFFICIENTLY REPRESENTED USING A COMMON CONSOLIDATION ALGORITHM?
Author: Nicholas Blauch
Thesis/Project Type: Independent Honors Thesis
Approved By: David E. Huber, Chair. Dept. of Psychological and Brain Sciences.
Approved By: Rosie A. Cowell, Committee Member. Dept. of Psychological and Brain Sciences

"Grid cells" in the medial entorhinal cortex (MEC) are proposed as the GPS coordinates in the computation of self-location downstream in the hippocampus (HC), where individual "place cells" fire in a specific place in an environment. To account for findings contradictory to this model, Huber & Solstad have proposed an alternative Memory-Retrieval Model of grid cells (submitted), which frames the grid response as the result of feedback from efficiently consolidated hippocampal episodes. The optimal consolidation algorithm is proposed as a universal consolidation algorithm in a representational hierarchical view of the brain, where different regions perform fundamentally similar operations on different types of information. Thus, we suggest that navigation in non-spatial perceptual and conceptual spaces will yield a grid-like signal in the cortical areas dedicated to processing these stimulus dimensions. To evaluate this proposal, we design a human functional magnetic resonance imaging (fMRI) study to test for the presence of a grid-like signal in visual cortex in response to "navigation" in a perceptual color space. Here, I analyze behavioral color similarity ratings in order to compute an individual's 2D perceptual color space, and analyze BOLD similarity patterns in order to compute a 2D cortical color space, both of which can be used to calibrate analyses of the grid-like pattern. While the behavioral experiment yields reasonable perceptual color spaces, we determine that more neuroimaging data needs to be collected both to compute cortical color spaces, and to test for grid-like responses to navigation in color space.

Table of Contents

1. INTRODUCTION

1.1. Memory and Spatial Navigation in the Medial Temporal Lobe

A fundamental question in neuroscience concerns how the brain codes for where we are in an environment, information which is necessary for spatial awareness and navigation in animals. Indeed, the neural coding of physical space has received extensive study over the past 50 years, and many crucial discoveries have been made. Scientists now understand that the hippocampal formation — including the hippocampus, entorhinal cortex, and subiculum — is crucial for an animal's ability to navigate physical space (O'Keefe & Nadel, 1978; Moser, Kropff and Moser, 2008). Studies in humans have revealed that these same brain regions underlie declarative and episodic memory (Squire & Zola-Morgan, 1991). Thus, it is of great interest to understand the representations stored and the computations performed in these areas of the brain, so as to connect our understanding of abilities ranging from spatial navigation to episodic memory. In understanding these brain regions, single-cell electrophysiology has been vital, whereby neuroscientists investigate the firing properties of individual neurons during a wide range of behavioral, cognitive, or perceptual tasks (e.g. O'Keefe & Dostrovsky, 1971; Taube et. al, 1990; Fyhn et. al, 2004).

Researchers have demonstrated the existence of several classes of cells relevant to spatial cognition: "head-direction cells," which respond when an animal's head faces a certain direction and are found in several regions, including the pre- and post-subiculum (Robertson et. al, 1999; Taube et. al, 1990) and the medial entorhinal cortex (Giocomo et. al, 2014); "boundary-vector cells," which respond when an animal is a fixed distance from an environmental boundary and are found in the subiculum (Lever et. al, 2009) and the entorhinal cortex (Solstad et. al, 2008); "grid cells," which respond when an animal is located on the vertices of an imaginary hexagonal

grid tiling an environment, and are found in the medial entorhinal cortex (Fyhn et. al, 2004; Hafting et. al, 2005); and finally, "place cells," which respond whenever an animal is at a given location in an environment and are found in the hippocampus (O'Keefe & Dostrovsky, 1971; O'Keefe & Nadel, 1978). Together, these cells seem to constitute the neural basis of spatial cognition. However, despite an accounting of these functional cell types, scientists have yet to ascertain the specific neural computations performed by these cells and within these brain regions, and how these neural computations contribute to cognition and behavior.

Attempts to formulate an understanding of these neural computations are formalized in mathematical or neural network models. One influential model explains the spatially-selective firing fields of "place cells" in terms of a linear combination of the firing fields of a population of spatially periodic "grid cells," which vary in position, orientation, and spatial frequency (Solstad, Moser & Einvole, 2006). This modeling framework might well be considered the standard model of the neural computation of place, culminating in a 2014 Nobel Prize Award in Medicine or Physiology, which touted entorhinal grid cells as the brain's "GPS coordinates," which allow the brain to represent place in the hippocampus. However, despite this high honor, in her Nobel Lecture, May-Britt Moser left room for the contributions of other cells in the computation of place, including boundary-vector cells and speed cells in the entorhinal cortex.

While the standard model is attractive in providing a mechanism by which absolute spatial location can be computed in the hippocampus by utilizing the inputs of spatially-periodic cells in the immediately upstream entorhinal cortex, recent evidence in experimental in theoretical neuroscience casts doubt on the plausibility of such a mechanism. First, deactivating the hippocampus of rodents results in the elimination of gridded firing fields in entorhinal "grid cells." (Bonnevie et. al, 2013). This finding suggests that grid fields in the entorhinal cortex are

in some manner dependent on hippocampal feedback to the entorhinal cortex. Secondly, in newborn rat pups first exploring an environment, stable place fields in hippocampal neurons develop before stable grid fields in entorhinal neurons (Bjerknes et. al, 2014). This finding suggests that non-grid cell inputs are sufficient to compute place, further questioning the role of grid cells in the feed-forward computation of place. These findings do not conform to the narrow bounds of the standard model, whereby place fields are generated solely from grid fields, which are generated from upstream (undiscovered) cells with spatially repeating receptive fields. A notable alternative model of place field formation — the Boundary-Vector Cell model (Hartley et. al, 2000; Barry et. al, 2006) — does not suffer from these issues, accounting for the computation of place using the inputs of boundary vector cells. However, all models so far discussed share a notable drawback: they fail to account for the role of the Medial Temporal Lobe in episodic memory, assuming that the functional roles of its dominant cell types are purely spatial. A new theoretical and computational framework for memory and spatial navigation in the Medial Temporal Lobe is needed.

1.2. A Memory Retrieval Model of Grid Cells

In two separate, unpublished conference proceedings, David Huber and Trygve Solstad introduced the memory-retrieval model of grid cells. They contrasted their new proposal with two existing model classes, as shown in Figure 1.

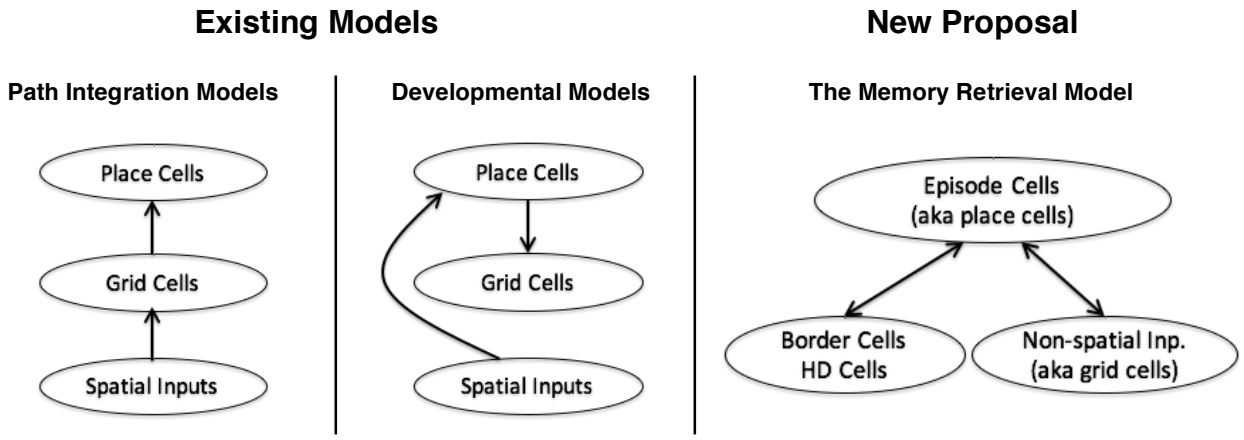

Figure 1. Grid Cell Models. Adapted from Huber & Solstad, 2016.

On the left are typical path integration models, in which spatial information derived from sensory inputs drives the formation of spatially-repeating grid cells, and grid cells are used to generate place cells (e.g. Fuhs and Touretzky, 2006; McNaughton et al., 2006; Solstad et al., 2006). In the middle are developmental models in which grid cells are derived from place cells, but the role of grid cells is unspecified (i.e. the proposal of Bonnevie et. al, 2013). On the right is the memory-retrieval model of grid cells. In this model, border cells and head-direction cells provide purely spatial information as a basis of building a spatial cognitive map in the hippocampus. Since the hippocampus is also necessary for non-spatial memory, the model includes non-spatial inputs feeding into the hippocampus, called "context cells," which measure contextual properties that are typically constant in the bland 2D boxes explored by rats in grid cell experiments. In the 17th century, Johannes Kepler conjectured that there could be no denser way to pack spheres than the hexagonal close-packed solution; only recently has this conjecture been formally proved and accepted as a theorem (Hales, 2005). In the space of a bland 2D box, the only features which are strongly modulated during navigation are X and Y position, and head-direction – thus the task of the hippocampus is to represent episodes in a 3D space. Rather

than storing a place field centroid at every possible location, which would require many neural resources, Huber & Solstad suggest that the hippocampus approximates the optimal hexagonal close-packed solution. The result is that, in the subspace of X and Y location, the centroids of hippocampal episodes are located along the vertices of a hexagonal grid. The model of Huber & Solstad approximates this solution via a novel simplex consolidation algorithm. As a rat navigates a box, stable, consolidated place fields are activated. Strong hippocampal feedback is implemented in order to retrieve the features which were active during memory encoding, and results whenever a hippocampal episode is remembered. Since context is constant, and hippocampal feedback is strong, "context cells" are driven by the gridded layout of hippocampal place cells, and respond with a "grid cell" response. Similarly, when a rat is headed in a given direction aligning with the preference of a head-direction cell, strong hippocampal feedback results in head-direction cells responding with a conjunctive head-direction/spatially gridded response.. Thus, the memory-retrieval model explains the presence of grid fields in medial temporal lobe neurons, and reconciles the role of MTL in both spatial navigation and memory in a single computational model.

1.3. The Representational-Hierarchical Account of the Brain

The representational-hierarchical account of the brain contrasts with modular views of brain function (e.g. the hippocampus "does" memory or spatial navigation) by instead describing the brain as deriving increasingly complex stimulus representations through successive, hierarchical processing stages proceeding from perceptual inputs and into the associative and "memory" areas of the brain (e.g. Cowell, Bussey & Saksida, 2006). The idea of hierarchical processing in the visual system is not new, dating back to the seminal work of Hubel & Wiesel (1968). However, the representational-hierarchical account provides a plausible connection point

between the typically separated domains of perception and memory, where memory is not a separate domain but rather the top of an increasingly complex hierarchy. This account, thus, does not discriminate between regions by proposing different computations and functions, but rather based on the representational complexity, and when relevant, the sensory mode involved (i.e. visual, auditory, associative). A representational-hierarchical view of the brain suggests that the operations performed between stages of the hierarchy may be the same regardless of which stage of the hierarchy is examined. Thus, we predict that the same consolidation process proposed to occur in the hippocampus for the representation of high-level spatial and memory features may be implemented at each stage of hierarchical cortical processing. If other "spaces" of brain representations are efficiently stored according to the hexagonal close-packed solution, we predict that a grid-like signal may be found in response to navigation through these other spaces.

In evidence of this notion, Constantinescu et. al (2016) demonstrated a striking grid-like response to navigation in a non-spatial 2D conceptual space. In their conceptual space, the neck and leg length of birds were changed continuously along certain trajectories. To test for a grid-like signal, the authors utilized a technique pioneered by Doeller, Barry, and Burgess (2010) to detect a spatial grid cells using human fMRI. Their technique capitalizes on three properties: 1) for activation which is determined along a hexagonal grid in a 2D space, activation is modulated by a sixfold-symmetric sinusoid of the running direction, 2) neighboring grid-cells share a common grid orientation and thus yield a stable macroscopic grid orientation amenable to discovery with spatially coarse fMRI, 3) neural adaptation. Thus, a grid-like signal can be measured in two ways: 1) sixfold-symmetric modulation of the BOLD signal, and 2) greater adaptation of the BOLD signal when a target navigation is preceded by one in a direction a multiple of 60° from the target navigation. A grid-like signal was found to navigation in the

virtual arena using both measures, the first evidence of spatial grid cells in humans using non-invasive fMRI (Doeller et. al, 2010). Whereas in rodents grid cells have been noted in the medial entorhinal cortex and subiculum, in humans, the grid-like signal was found in a large network of regions, including entorhinal, medial prefrontal, parahippocampal, retrosplenial, lateral temporal, and posterior parietal cortices. That the grid-like signal in fMRI reflects the presence of underlying grid cells has since been confirmed using direct recordings on the brains of neurosurgery patients (Jacobs et. al, 2014).

In Constantinescu et. al (2016), the same approach was used to detect a grid-like signal, only navigation occurred in a conceptual space. Participants were taught to associate specific neck and leg length combinations (i.e. exemplars in bird space) with different reward symbols. After training, participants were placed in an fMRI scanner, and were exposed to navigations in bird space and asked to predict which bird (associated with a specific symbol) the bird was morphing into. The study revealed sixfold-symmetric modulation of the BOLD signal, in many of the same areas as in Doeller et. al (2010), namely, the entorhinal and prefrontal cortices, and also orbitofrontal, posterior cingulate, retrosplenial, lateral parietal, and temporoparietal cortices. In both studies, a much broader network of regions was found to exhibit a significant grid-like signal than had been predicted a priori, according to a standard feed-forward model of grid cells. In our view, this adds strength to the memory retrieval model; rather than supposing that several regions feed forward a separate grid code of spatial/cognitive/memory features, it is more parsimonious to presume that each of these regions receives strong feedback from the hippocampus, with the grid-like signal reflecting memory retrieval of episodes organized along a grid after consolidation.

To our knowledge, no study to date has demonstrated evidence for a grid-like signal in early perceptual areas. In testing the memory retrieval model of grid cells in the context of a representational hierarchical view of the brain, we seek to determine whether there are distinct populations of cells responding with a grid-like signal at such earlier stages of perceptual processing. A representation of color exists in early visual cortex and is passed into successive regions of the ventral visual stream. The color inputs to primary visual cortex can be defined along two dimensions of chromaticity and one dimension of luminance, where each channel is determined by the outputs of retinal cones (Derrington, Krauskopf & Lennie, 1984). Thus, the chromaticity of a color serves as a suitable 2D space for testing for the existence of a gridded response along non-spatial dimensions, in regions outside of the hippocampal formation. Color spaces and their neural representations are discussed in detail in the next section.

1.4. The Neural Representation of Color

Information on color is achieved in the earliest stage of photo-reception in the retina with the presence of three separate cone photoreceptor types, each responding to color with a different spectral response profile; these cones are thus termed short (s), medium (m), and long (l) cones for the wavelength which maximally activates them. These cone activations serve as the basis set of color information in the visual system. In the perception of color, this basis set of information is transformed along the pathway from the retina, to the lateral geniculate nucleus of the thalamus, to primary visual cortex, and along the visual cortical pathways (Solomon & Lennie, 2007). In the retina, cone signals are combined in retinal ganglion cells in a center-surround fashion akin to the achromatic center-surround receptive fields present in other retinal ganglion cells (Solomon & Lennie, 2007). These receptive fields receive input from one type of cone in the center of their receptive field, and from another type of cone in the circular surround. As

such, these cells are able to detect color contrasts (Solomon & Lennie, 2007). In the lateral geniculate nucleus (LGN), the activities of retinal ganglion cells are combined to produce two color opponent chromatic channels and a luminance channel (Derrington, Krauskopf, Lennie, 1984). The combined activation of these three channels may fully specify the color of a stimulus, and can be transformed to RGB space and other color spaces. Derrington, Krauskopf, and Lennie thus termed the space of these channels DKL space, which they derived from the 2D cone-chromaticity diagram of Macleod and Boynton (MB space) (1978). Because activation of the s cone has been demonstrated not to contribute to luminance perception (Eisner & Macleod, 1980), the luminance dimension in MB and DKL spaces is defined as (l+m), the summed activation of l and m cones. Whereas MB space defines a 2D cone-chromaticity diagram in terms of l/(l+m) and s/(l+m), DKL space introduces a small modification in order to match the chromatic dimensions to the chromatic channels found in LGN, setting the chromatic dimensions to (s) and (l-m). These chromatic dimensions are thought to represent the chromatic input to primary visual cortex. Owing to its physiological relevance as a model of the color space representation in LGN, and its isoluminant 2D chromatic subspace, DKL space serves as an excellent candidate color space for testing whether there are neurons which respond to non-spatial 2D spaces along a grid. However, it should be noted that other color spaces with an isoluminant 2D chromatic subspace (e.g. MB, CIELAB) may work equally well.

Despite a tractable understanding of the representation of color in the early perceptual stages of the retina and lateral geniculate nucleus, the nature of color representation in the cortex, where the bulk of complex visual processing is performed, is less fully understood. A still unresolved issue concerns the degree of separability in the processing of form and color. One view suggests that cortical color processing proceeds relatively independently from form

processing, until form and color are bound at later stages of processing. This view has been advanced at several levels of analysis. At the behavioral level, visual search paradigms have been interpreted in the context of Feature Integration Theory to demonstrate parallel processing of color or form stimuli but serial processing of color/form conjunctive stimuli, suggesting that color and form are represented as separate features (Treisman & Gelade, 1980). At the level of brain regions, Zeki (1973) proposed that area V4 is the site of color processing, Hubel & Livingstone (1977, Livingstone & Hubel, 1978) demonstrated distinct patches in V1 and V2 selective for color, and recently, the existence of a distinct set of color-selective patches has been demonstrated along the ventral visual stream of macaque monkeys (Conway, Moeller & Tsao, 2007), situated between face and place selective regions (Lafer-Sousa & Conway, 2013); a homology has been demonstrated in humans, with a similar set of color-selective patches similarly situated between face and place selective regions (Lafer-Sousa, Conway & Kanwisher, 2016. Such an organization, presumably, would allow for color to be flexibly bound to mid- or high-level form constructions.

The modular view of color representation in the cortex is, however, far from unopposed (Shapley & Hawken, 2011; Rentzeperis et. al, 2014). One important finding demonstrated that, in line with the modular view, cells in early visual cortex prefer either color or form, with their mean response in a time window immediately following stimulus presentation yielding information about one of these dimensions (McClurkin & Optican, 1996). However, the crucial difference is that this study chose to analyze their neural data in an additional way; these authors analyzed the information content present in the time course of neural activation, and in so doing, demonstrated that cells selective for color or form typically also contained information about the other stimulus dimension in the time course of their activation; in fact, the information present in

the time-course of activation was much greater than that present in the mean response, supporting a likely function in neural processing. The exact neural mechanisms by which such a multiplexed signal is generated or read out remain to be fully elucidated. One possibility is that the feed-forward response of such cells is the stimulus dimension for which information is present in mean response, as studies claiming dedicated color representation have suggested, and the time course information for the orthogonal stimulus dimension represents feedback from higher conjunctive representations. Thus, we think it worthwhile to examine further the combined selectivity of neural populations to color and form, examining this selectivity from the perspective of a general cortical representational scheme in which conjunctive representations are efficiently consolidated, and in which feedback may provide important characteristics to the firing patterns of lower level neurons.

In any case, this study is unconcerned with the particular localization of color, form, and their conjunction in the brain. Our analyses are not targeted to any specific region of interest, but rather, are sensitive to effects appearing anywhere in visually responsive cortex. In attempting to observe a sixfold-symmetric neural response in a 2D space orthogonal to the neuron's feed-forward receptive field, the necessary requirements are 1) that color and form are represented largely separately in earlier regions, 2) that downstream neurons receive inputs from both populations, possessing a multidimensional response sensitive to form and color (but not necessarily a specific conjunction), and 3) that these downstream neurons send feedback signals to the earlier neural populations that represent color and form largely separately. We believe that requirements 1) and 2) are well born out in the literature, as discussed above, despite some evidence for overlap in early processing of form and color. We expect that requirement 3) is likewise met, given the presence of feedback projections throughout visual cortex; however, the

precise contribution of high-level feedback to the responses of early visual neurons is not fully understood. Reconciling the finding that neurons selective to either color or form in mean response are selective for both in the temporal distribution of their response, we suggest that this may be the result of specific feedback from higher-level neurons whose mean response demonstrates selectivity for both color and form.

2. ORIGINAL RESEARCH

In this section I will discuss the methods and results of a behavioral/psychophysical experiment designed to map an individual's perceptual color space, and of a neuroimaging experiment designed to both map an individual's cortical color space and to test for grid-like responses in visual cortex to navigation in color space.

2.1. Methods

2.1.1. Implementing DKL Color Space

The color space of Derrington, Krauskopf, and Lennie (1984) (DKL space) was used to create isoluminant colored stimuli determined by two dimensions of chromaticity. Where *s*, *m*, and *l* are the cone activations of short, medium, and long cones, respectively, luminance is defined by *l*+*m* and an isoluminant color plane is determined by the chromatic coordinates *s* and *l*-*m*. In calibrating the DKL color space, the spectral radiance profile of a monitor was determined using an ILT 350 spectroradiometer (International Light Technologies, Peabody MA). Readings were taken for the lab computer monitor (ASUS VG248) used in the behavioral experiment, as well as for the BOLD monitor used in the neuroimaging experiment. Gamma correction was performed on the lab computer monitor using a color look-up table generated from illuminance measurements taken with the spectroradiometer. For the BOLD screen, gamma correction was performed automatically with a factory-set script which calls a color look-up

table generated from factory measurements. Gamma correction was verified by checking for linearity in illuminance measurements across linear changes in intensity values. For all monitors, the Stockman, Macleod, and Johnson (1993) cone fundamentals were used to compute cone activation values given a spectral response of a monitor.

For each monitor, we calculated the maximum color reproducible disc from which to draw stimulus color values in behavioral and neuroimaging experiments. A background intensity value on 0-255 was used to set each value of the background RGB coordinates. Background RGB coordinates were transformed into DKL space, and the chromatic coordinates were set as the origin of an isoluminant plane, given as $O = (o_{l\text{-}m}, o_s)$. DKL values were transformed to RGB along the vertical *s* dimension until an invalid RGB vector was created; invalidity was determined if any of the R, G, or B values were less than 0 or greater than 255. The maximum monitor producible radius was saved for the *s* dimension, referred to as r_s. The same process was performed along the horizontal *l-m* dimension, achieving a radius $r_{l\text{-}m}$. To maximize the area of an isoluminant plane, DKL coordinates were scaled such that the maximum square plane contain *l-m* values on $[o_{l\text{-}m} - r_{l\text{-}m}, o_{l\text{-}m} + r_{l\text{-}m}]$, and *s* values on $[o_s - r_s, o_s + r_s]$. Because we used a numerical programming language (MATLAB) rather than continuous mathematics, discrete increment values were chosen to compute points along a dimension in color space; thus, scaling was achieved by modifying the increment values i_s and $i_{l\text{-}m}$. To create 60 frames along a radius in color space, the increment values were modified such that $60 * i_s = r_s$ and $60 * i_{l\text{-}m} = r_{l\text{-}m}$. Using these increment values and a maximum radius of 60 increments, the maximum radius was swept along a perimeter in DKL color space at increments of 1°; at each point, a validity check of the RGB transformed coordinates was performed. In the case that an invalid RGB value was found, the radius was decremented, and the search resumed at the same angle. This process was

performed until a radius was found, in number of increments n_i, at which all angles tested were valid. Both increment values i_s and $i_{l\text{-}m}$ were multiplied by (n_i / 60) to yield new increment values i_s and $i_{l\text{-}m}$ allowing for 60 radial increments to be validly computed along any polar angle in the isoluminant plane.

Thus, the implementation of DKL space takes a background intensity value on 0-255, and yields a 2D isoluminant disc containing valid DKL coordinates, specified by an origin O = ($o_{l\text{-}m}$, o_s), step radius = 60, and increment values i_s and $i_{l\text{-}m}$. I determine the increment values as a function of the brightness level, shown below.

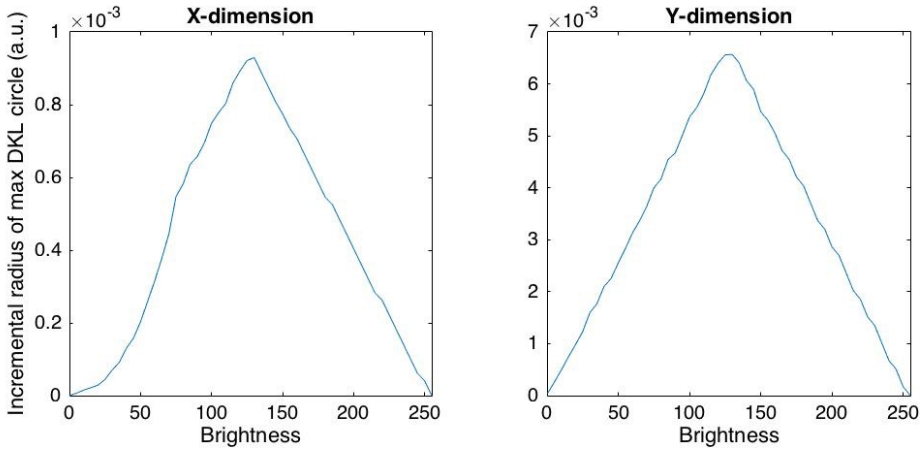

Figure 2. Length of DKL isoluminant disc radius as a function of brightness

From the above we determine that a brightness of 128 yields the maximum area isoluminant circle. The pattern is the same for both behavioral testing room monitors and the fMRI BOLD screen. Visual plots of the isoluminant circle and thin annulus are shown in Figure 3.

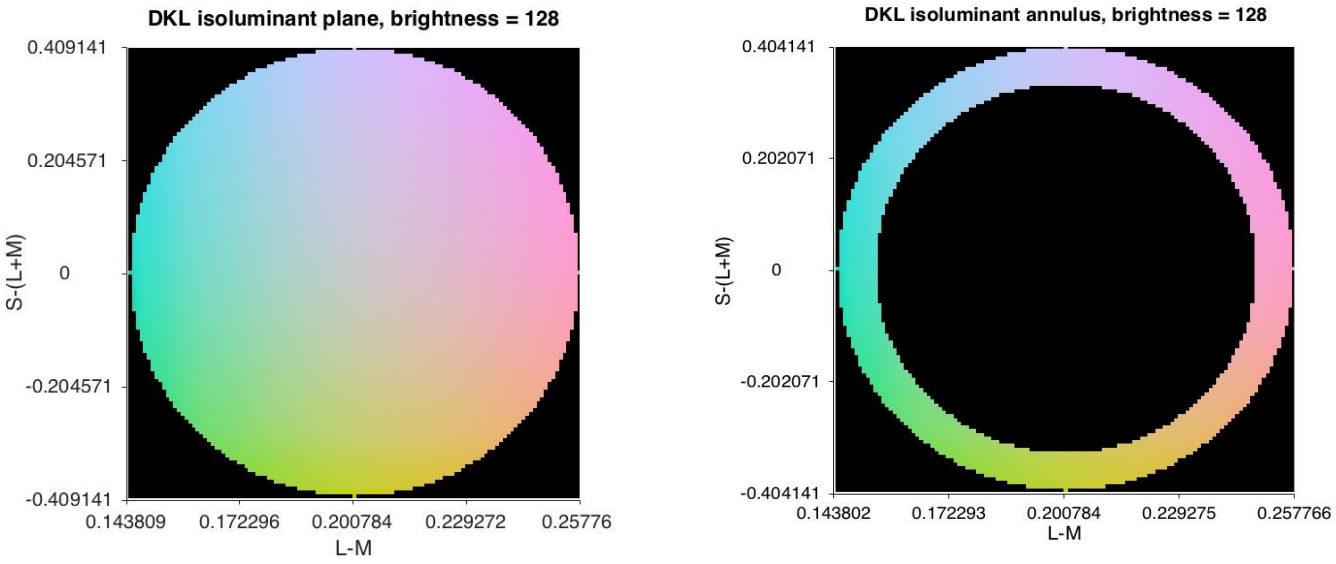

Figure 3. Isoluminant disc and annulus in DKL space

2.1.2. Behavioral experiment

The behavioral portion of this thesis involves a psychophysical experiment designed to create a 2-dimensional "map" of an individual's color space in advance of the fMRI experiment. Following verification of normal color vision using a minimal set of Ishihara plates (Ishihara, 1917), four healthy participants between the ages of 20 and 24 completed the behavioral experiment. Participants provided written informed consent. Experimental procedures were in compliance with an IRB protocol registered to David Huber and Rosie Cowell. Later screening considerations and technical issues for the fMRI experiment resulted in only two complete sets of fMRI data. Only behavioral data for the subjects who later successfully completed the fMRI experiment are shown in the Results section. First, 24 isoluminant colors are drawn from the DKL isoluminant color disc, generated for the monitors located in the lab's behavioral testing rooms. 24 colors are chosen along the disc's perimeter, beginning at 0 degrees from the horizontal and separated by 15 degrees in a polar reference frame. To determine an individual's

perceptual color space, participants perform a color similarity behavioral experiment, in which pairs of these colors are shown in boxes placed next to each other on screen for an indefinite amount of time. Participants are asked to rate the similarity of the 2 colors on a 1-7 scale, where 1 is "same", and 2-7 is "different", and increasing value corresponds to greater dissimilarity. Each participant completed 4 runs, where one run consists of one presentation of each possible color pair. Following data collection, for each participant, the mean pairwise color similarity ratings across runs are combined into an upper triangular dissimilarity matrix to be input to a multidimensional scaling (MDS) algorithm. MDS is performed using the *mdscale* function in MATLAB, setting the number of scaling dimensions to 2, in order to create a 2-dimensional perceptual embedding. This 2-dimensional perceptual embedding can be used to parameterize the analyses of the fMRI experiment, as discussed in the results section.

2.1.3. Neuroimaging Experiment

Participants who completed the behavioral experiment were subject to screening prior to completing the fMRI experiment using the standard screening procedure of the Human Magnetic Resonance Center at the University of Massachusetts, Amherst. Of the four participants who completed the behavioral experiment, one was screened from the fMRI experiment, leaving three healthy participants who completed the fMRI experiment. Of the three participants who completed the fMRI experiment, one participant's session was subject to some presentation timing problems. Thus, their data were not included in analyses.

A functional Magnetic Resonance Imaging (fMRI) study was performed in which participants viewed dynamic videos of colored visual stimuli, and rated the similarity of sequences of dynamic stimuli. A maximum area DKL chromaticity disc was acquired using the same method as in the behavioral experiment, calibrated to the BOLD-compatible monitor at the

UMass Human Magnetic Resonance Center (HMRC). However, rather than using only the perimeter of this disc, in the fMRI experiment, 24 radial paths from the disc center to perimeter points are used to create dynamic stimulus "trajectories" designed to optimally allow for our analysis methods to detect the presence of a hypothesized population of neurons responding to color along a hexagonal grid; the method for detecting a grid-like signal in fMRI (Doeller et. al, 2010) was described in paragraph 2 in section 1.3. Single image frames are generated along the radial trajectory from center to perimeter; 60 image frames are taken to accommodate a 1s visual presentation of the trajectory presented at 60 Hz. Creating such a trajectory for each of 24 colors yields a bank of 24 movies, each consisting of 60 image frames, as the full set of dynamic visual experimental stimuli. Stimuli were large chromaticity defined square-wave gratings, with the circular diameter subtending 15° of visual angle. Bars of the grating alternated between isoluminant colored and grey bars. Two orientations were used, vertical and horizontal, in alternating experimental runs. For this study, a single experimental stimulus consists of two repeats of a radius to perimeter trajectory, thus taking 2s. We use an event-related design in which a stimuli videos are played one after another including break periods and null trials. One trial consists of 2s of a dynamically colored grating stimulus followed by 2 s of an uncolored grey grating stimulus, as shown in Figure 4. Null trials consist of 4s of uncolored grating stimulus. An experimental run consisted of 16s of uncolored grating stimulus followed by 84 experimental trials. Of these 84 experimental trials, 5 were randomly selected to be null trials; null trials were constrained not be the first or last trial of a run, and null trials were placed with at least 2 color trials in between. The participant's task was to fixate the center of the stimulus and, on each trial besides the first, to rate the similarity of the color of the current trial with that of the previous trial, on a scale of 1-4. Participants made ratings while being scanned using 4 buttons

on a 5 button device. Experimental runs collected functional BOLD data with 3 mm^3 voxels, taking 44 slices along the dorsoventral axis with a 1.5s repetition time, yielding a time-course of 235 functional images of size 68x68x44. Experimental runs were split between vertical and horizontal orientation grating stimuli. Experimental runs were preceded by a high-resolution (1 mm^3 voxel size) anatomical scan, and were interspersed with two standard retinotopic localizer scans and three luminance-defined orientation-tuning scans.

BOLD images were pre-processed using SPM12 software, performing slice-time correction and realignment of functional images, as well as co-registration of the mean functional images to the high-resolution anatomical image, and finally segmentation of the co-registered functional images. To compute the cortical color space, a general linear model (GLM) was fit to the time-course of functional images for each run, using one regressor for each of 24 colors and additional motion correction covariates estimated during pre-processing. Applying the general linear model to functional data thus provides a beta-weight for every color/run/voxel combination, serving as the basis for further analyses. To perform decoding analyses, we increased the number of samples by fitting a GLM to each trial individually (Mumford et. al, 2012), yielding a matrix of beta-estimates across voxels for each trial, with a corresponding trial stimulus color, which could be used as predictors and labels for classification analyses.

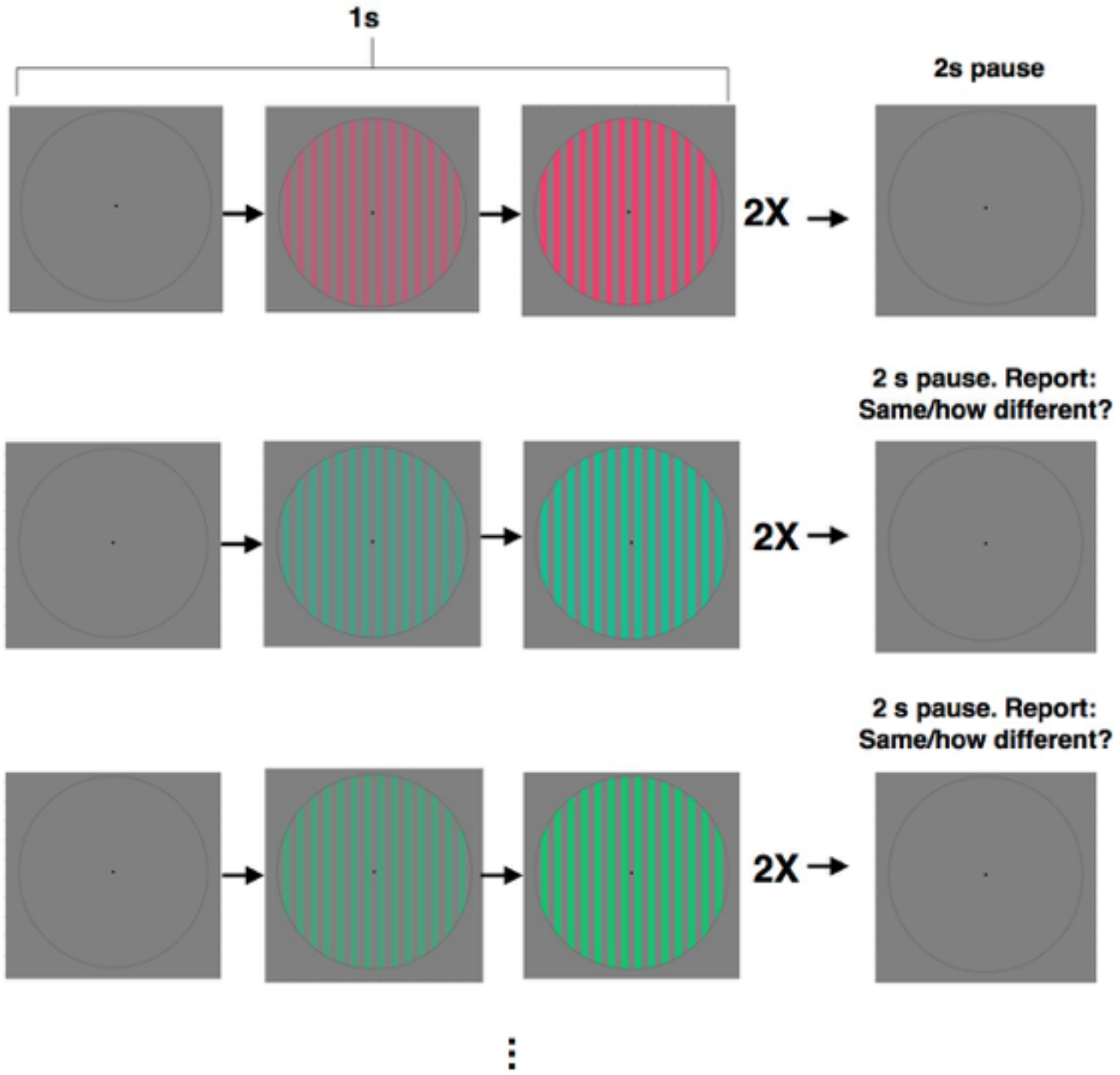

Figure 4. Stimulus time course. Stimulus begins with all gray bars, and then alternating bars saturate continuously to color 1 (1 s). Repeat. 2 s pause at gray. Repeat, saturating to color 2. Excluding the first trajectory, the participant rates the similarity of the preceding two colors on a same/how different scale of 1-4, where 1 is same and 2-4 are different, 4 being the most different.

2.2. Results

2.2.1. Behavioral Results: Mapping the Perceptual Color Space

Behavioral experimentation and analyses were carried out as discussed in Methods, section 2.1.2. For the two subjects who underwent later successful fMRI scans, the results of multidimensional scaling (MDS) of perceptual similarity ratings are shown in Figure 4. I also perform Procrustes transformations to the raw MDS solutions, a technique which generates the best fitting transformation composed of uniform scaling, translation, and rotation. The resulting Procrustes transformed MDS solutions are plotted below. Lines are drawn to connect neighboring points in the original DKL space.

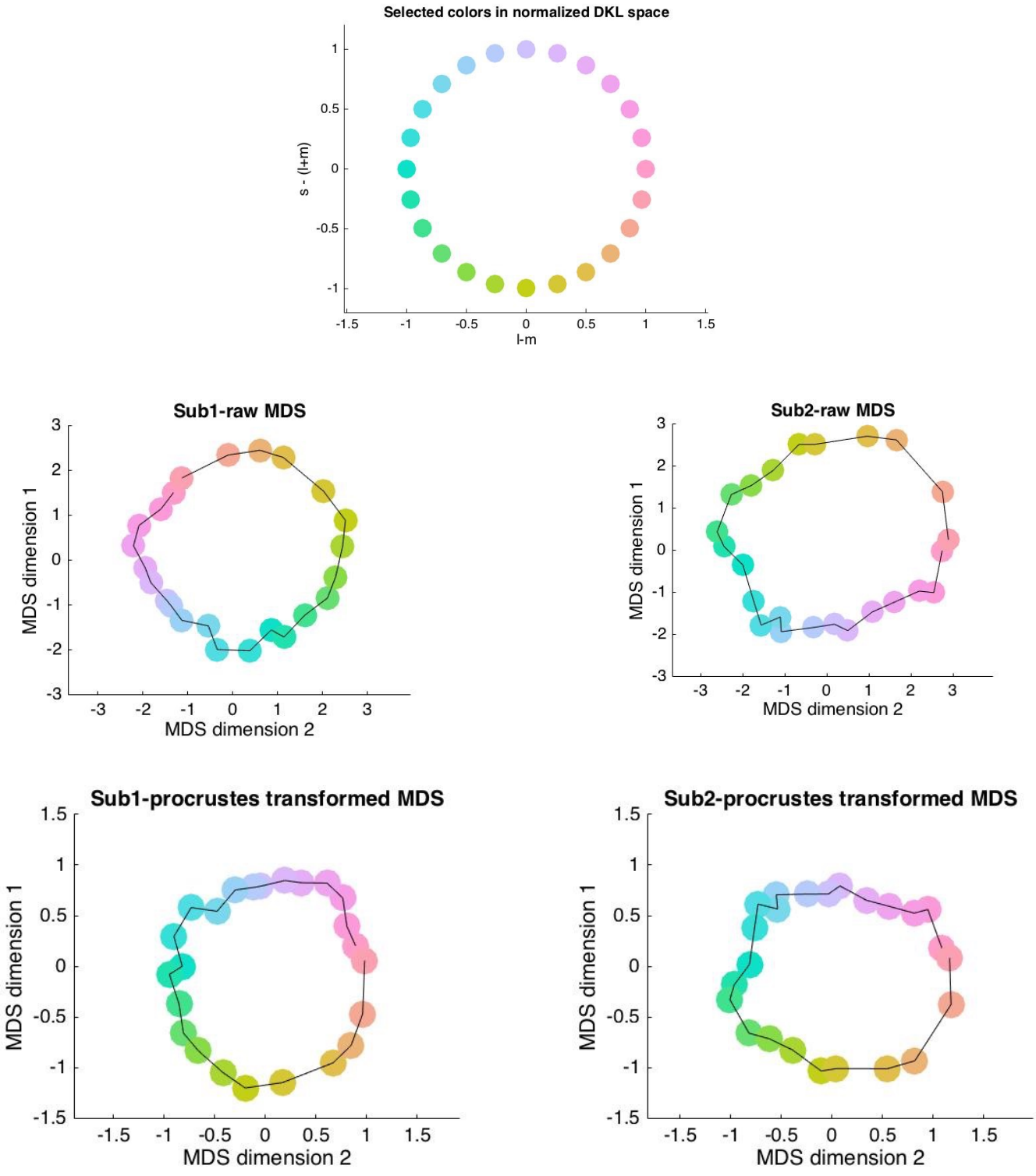

Figure 5. DKL space and perceptual color spaces

Finally, to achieve a set of perceptually defined angles in color space, the Procrustes transformed MDS solutions are converted to polar coordinates. For visual demonstration, the solutions are projected onto a circle defined by the max radius of the solution in polar coordinates. The radii of polar DKL coordinates is multiplied by 0.8 so as to plot the DKL circle within the perceptual circle.

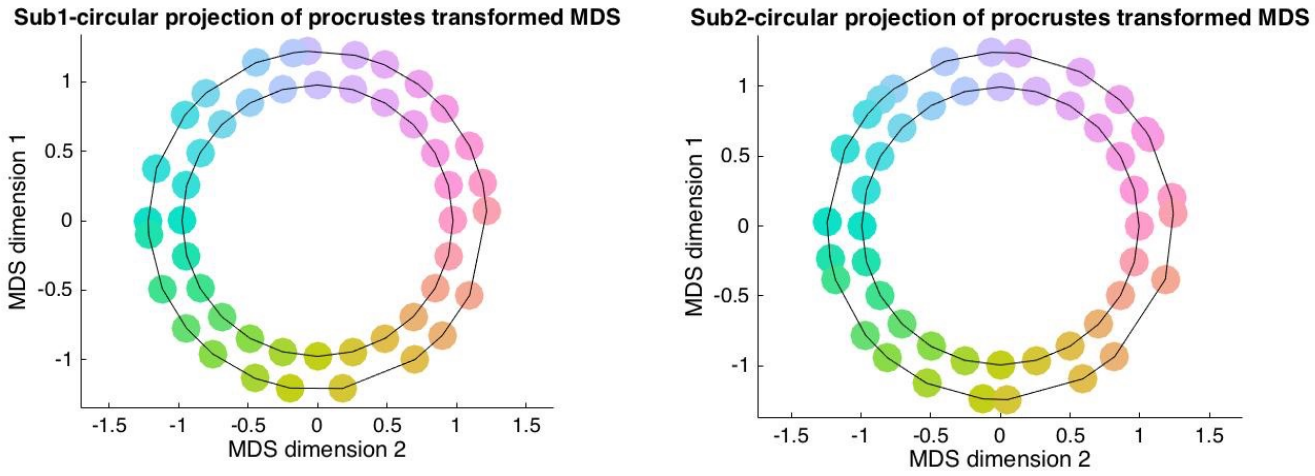

Figure 6. DKL space plotted inside the circular projections of perceptual color spaces

The resulting perceptual angles are plotted in the table below.

DKL Angles	Sub 1 Perceptual Angles	Sub 2 Perceptual Angles
0	12.7	9.3
15	26.1	30.6
30	41.3	32.9
45	53.4	46.5
60	66.7	62.4
75	77.1	84.3
90	93.4	92.9
105	98.3	108.7
120	111.4	127.9
135	131.2	133.5
150	141.6	139.9
165	161.9	153.8
180	180.0	178.7
195	184.9	190.7
210	203.7	198.1
225	219.3	218.9
240	231.6	229.3
255	248.3	244.8
270	260.7	264.1
285	278.5	272.3
300	305.1	298.4
315	317.4	311.2
330	333.9	342.2
345	3.2	4.1

Table 1. Angles of experimental stimuli in DKL space and circular projections of perceptual color spaces.

In the 2D perceptual spaces generated from multidimensional scaling of behavioral dissimilarity ratings, the relative circularity and ordering of points is preserved from the original DKL space, shown earlier. Generally, this confirms the notion that DKL space well organizes points in the perceptual color space. However, some discrepancies between the perceptual color space and the original DKL color space are seen. From projection, we can easily see that there is a bit of clumping in the perceptual color spaces, indicating that the perceptual polar angle difference between colors is not uniform across pairs of points, differing from the uniform difference as drawn from DKL color space. The generation of perceptually defined color angles allows us to utilize psychophysical data to calibrate further neuroimaging analyses, providing a potentially more useful parameterization of the color space than the original DKL angles. To do so, the DKL angles are replaced by the perceptual angle in symmetry analyses. However, sixfold-symmetry analyses were carried out by a post-doctoral researcher in the lab, and thus these analyses are not provided in this thesis.

2.2.2. Neuroimaging Results: Mapping the Cortical Color Space

We follow the same procedure for mapping the cortical color space as was done in mapping the perceptual color space. We derive a measure of dissimilarity from the coefficients of regression ("beta weights") acquired for each color in each experimental run. The correlations between vectors of beta weights for each color across runs are computed, yielding an upper diagonal correlation matrix, which is transformed to a dissimilarity matrix by subtracting each value from 1, such that colors which are maximally positively correlated have a dissimilarity value of 0, colors which are uncorrelated have a dissimilarity value of 1, and colors which are maximally negatively correlated have a dissimilarity value of 2. Before computing correlations, voxels were selected in terms of their responsiveness to color or orientation. Responsiveness was

computed as the p-value of a balanced 1-way ANOVA by group (e.g. color or orientation), after selecting for runs by orientation, or not. We show analyses selecting for voxels with significant responsiveness to orientation and color, irrespective of the orientation of stimulus presented, and additionally to color given horizontal or vertical orientations.

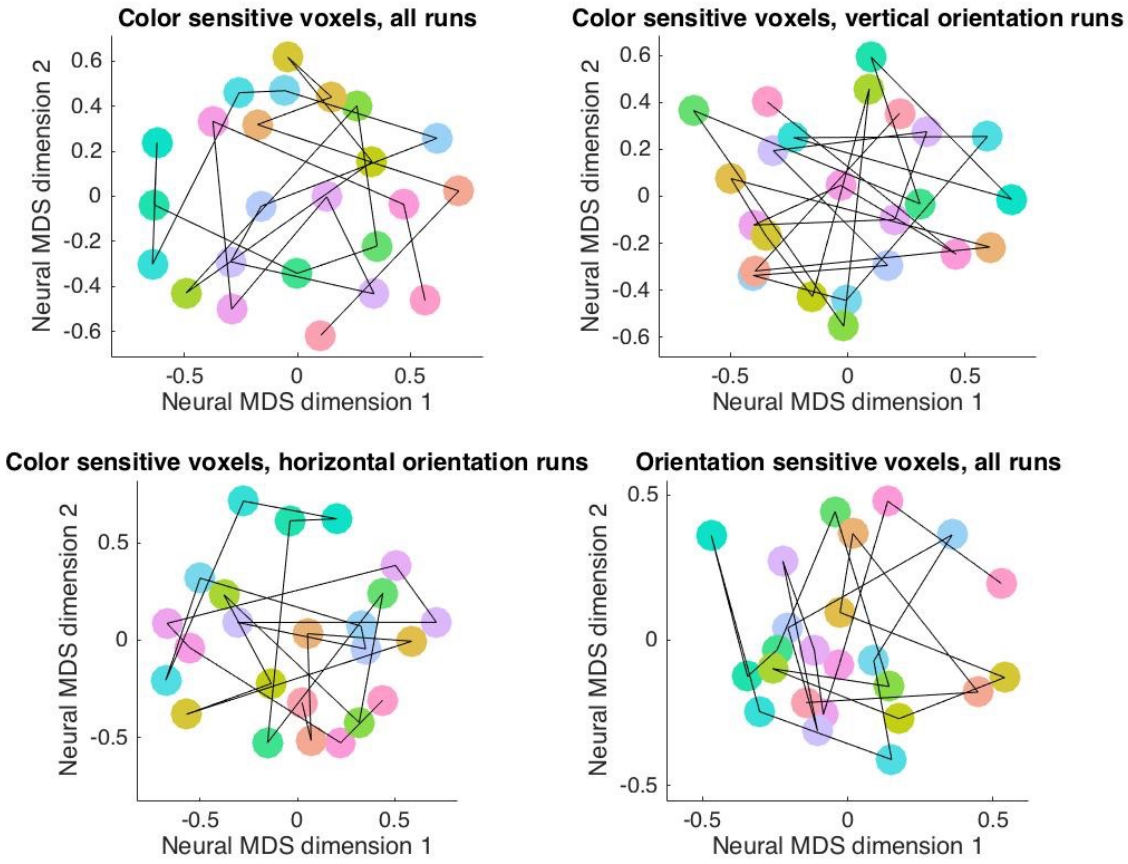

Figure 7. Cortical 2-D MDS solutions for subject 1.

As is clear from these plots, the BOLD data is much noisier than the behavioral data, and does not yield reasonable color spaces. Owing to this, we do not attempt to fine-tune the space with a Procrustes transformation, nor do we compute cortically derived angles in color space as was

done for the perceptual space. To quantify the color information present in the brain, we performed additional decoding analyses, discussed in the next section.

2.2.3. Neuroimaging Results: Decoding the Cortical Color Space

To perform decoding analyses, we began with a trials x voxels matrix of trial-specific GLM beta-weights. We selected for voxels in the same ways as in the previous section, using the same voxels which were acquired from analyses of variance on the run-specific GLMs. Decoding was performed using multi-class, 10-way cross-validated support vector machine-based systems, using the *fitcecoc*, *crossval*, and *kfoldLoss* functions in the MATLAB Statistics and Machine

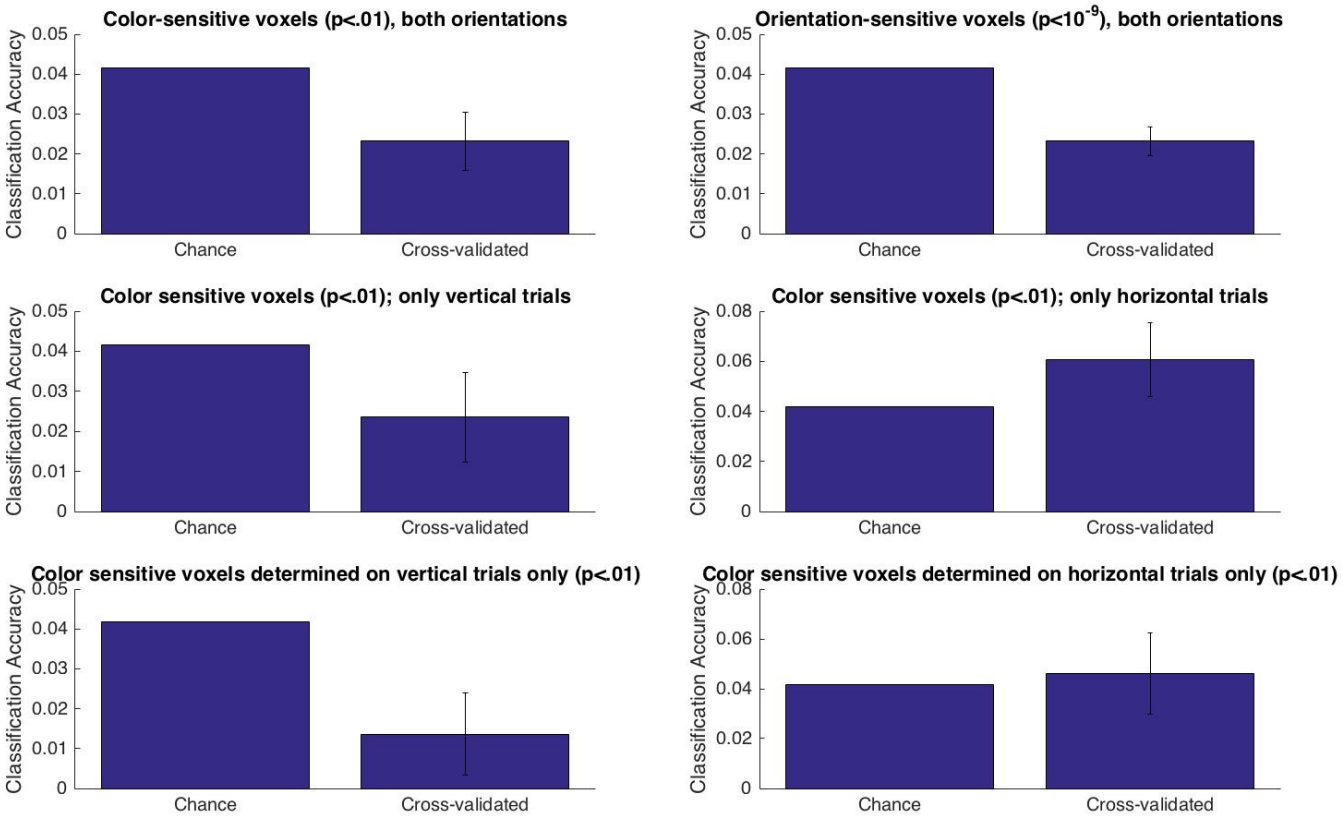

Figure 8. Decoding color from cortical activation patterns of subject 1. Voxels and trials of analysis are selected as specified in subfigure titles. The mean accuracy across cross-validated classification of 10 folds of 20% test data are reported, with an error bar corresponding to the standard error of accuracy across folds.

Learning toolbox. Classification accuracy is reported as 1 - mean loss across folds, and standard error is reported as the standard deviation of (1-loss) across folds divided by the square root of (number of folds – 1). Decoding results are shown in Figure 7.

The decoding results match the unreliability of the earlier mapping results. Only one decoding analysis achieves significance: decoding color using color sensitive voxels (determined using all data) applied only to horizontal orientation trials.

4. General Discussion

The neuroimaging data collected for this study proved to be largely unreliable, failing to generate a reasonable cortical color space or to yield significant decoding performance. There are at least two possible reasons for this. The first and, we believe, primary reason for unreliable cortical color responses is the small amount of data that was collected per color, per subject. In a study where a reasonable color space was acquired from BOLD data, Brouwer & Heeger (2009) used only 8 colors, with 3-5 sessions per subject, whereas we used 24 colors with only 1 session per subject. Thus, their study collected roughly 9-15 times more data per color, providing them with additional statistical power to uncover the cortical color space from noisy, coarse-grained blood oxygenation data. In future work, we plan to collect more data per subject to allow for high-powered within subject analyses, likely necessary to recover a color space containing as many colors as we would like to include to provide maximal flexibility for the analyses of sixfold symmetry. In this future work, we will also perform analyses of sixfold symmetry, in order to test the memory-retrieval model of grid cells in the context of a representational hierarchical view of the brain. The second possible reason for an unreliable cortical color space is that our experimental protocol, in which color was presented along dynamic trajectories from a central gray point to a radial point in a circular isoluminant color plane, induced an unstable

neural response. To our knowledge no study to date has examined this type of dynamic color stimuli using fMRI. Thus, it may be useful to compare our findings with data collected in-house using stimuli in which color saturation is constant in time.

A main theoretical hurdle that the memory retrieval model of grid cells must clear is determining the role of strong feedback from high-level conjunctive areas (e.g. HC) to lower-level areas (e.g. MEC), both in the hippocampal formation as well as in other areas (e.g. visual cortex) proposed to contain sixfold-symmetric responses owing to higher-level feedback of efficiently consolidated representations. In the model, such strong feedback is necessary to develop gridded responses in head-direction or "context" cells. In the hippocampal-entorhinal circuit, the role of feedback seems plausibly to activate the features which were active during the encoding of the episode. However, in predicting a grid-like response in earlier visual regions, the role of this type of feedback is less clear. The representational hierarchical account of the brain offers a parsimonious approach to studying the brain, whereby the operations are fundamentally similar throughout the brain, operating on different types of representations. However, if the memory retrieval model of grid cells proves to be correct in its characterization of the mechanism underlying sixfold spatially symmetric responses in MEC neurons, the same level of feedback implicit in this mechanism may not be present in other brain regions, even if the same consolidation algorithm is applied, consistent with the representational hierarchical account but inconsistent with our prediction of a sixfold symmetric response to navigation in color space.

Possibly the most challenging consideration in detecting a grid-like response at a 3 mm^3 resolution BOLD signal is that summation of the activity of hundreds of thousands of neurons over such a large region (i.e. that of a voxel) might hide any underlying gridded responses. The reason that the technique developed by Doeller, Barry, and Burgess (2010) is able to detect

spatial grid cells is that neighboring grid cells share a common grid orientation. Without such a common grid orientation at a macroscopic scale, putative color "grid cells" would not be detectable with this technique. A more sensitive technique for testing our hypothesis would utilize single-cell electrophysiology, in which neural activity is directly recorded.

A substantial body of research into cortical color coding has been conducted utilizing direct neural recordings. Some studies have characterized neurons in visual cortex (e.g. Wachtner, Sejnowski & Albright 2002; Conway, Moeller, Tsao 2007) as a function of hue in an isoluminant color space. Neither of these studies demonstrated evidence for neurons possessing a multimodal response in hue space (as would be true of the 'color' grid cells predicted by the memory-retrieval model); rather, most neurons tended to prefer a specific hue. Conway, Moeller, and Tsao (2007) observed "modules" containing color-selective neurons, which they detected using fMRI by measuring the selectivity of voxels for chromaticity-defined gratings vs luminance-defined gratings and storing the coordinates of significant voxel clusters. They then targeted these modules, which they call "globs," using single-cell electrophysiology, measuring the shape and color selectivity of neurons in globs, and "inter-globs," the space in between globs. For color selectivity, 45 hues were presented, placed evenly around a hue circle equivalent to the one used in our experiments. In globs, most cells were selective to one hue invariant of luminance, as well as for the orientation and length of the bar. In inter-globs, cells were more strongly selective for orientation and length of a colored bar, and few demonstrated some color selectivity, however this color selectivity was not invariant to luminance. While none of the cells shown displayed sixfold symmetry in their hue response, it is possible that the metrics used for color selectivity overlooked these cells, owing to a preference for selecting cells with a unimodal response profile. Selectivity was defined in two ways: the Rayleigh vector length, which is large

for a strong unimodal response and zero for an evenly (e.g. sixfold) symmetric response, and the color-to-achromatic response ratio, which is large for a strong unimodal response, and could be large or zero for an evenly symmetric response, depending on the baseline of the symmetric function. For example, a sixfold-symmetric neural response defined by a regular sine wave with a wavelength of 60 deg in hue space and mean response set at the baseline firing rate would yield zero color selectivity in both measures, due to the negative impact of troughs on measures of color selectivity incorporating the full range of hue values. Thus, while it seems unlikely that the authors of these single-cell studies would have overlooked the responses of "gridded" color cells, if their analyses tended toward the application of objective measures and away from visual inspection, it is very possible that the color selectivity measures used caused them to fail to detect such cells. Since their experiment, though possibly not their analyses, was well designed to detect gridded color neurons, a fruitful line of inquiry in this work may be to reanalyze their data to explicitly test the hypothesis of color grid cells. Given their experimental design, if cells exist in visual cortex with a sixfold symmetric response in an isoluminant color space, this reanalysis should reveal their presence.

Another possibility is that the memory retrieval model is correct that feedback from retrieved memory episodes stored in hippocampal representations is the source of grid fields in medial entorhinal neurons, but this consolidation – or sufficiently strong feedback – occurs only at this top level of the hierarchy, and not at other intermediate areas. In such a case, using an active version of our experiment in which participants must covertly use knowledge of the relationships between elements of the 2D color space, we might replicate the findings of Constantinescu et. al (2016) of grid-like responses in regions of the hippocampal formation and other frontal regions, but fail to find grid-like responses in visual cortex. This finding would add

support to the notion that the hippocampal formation is flexibly recruited to represent both conceptual (e.g. perceptual) and physical spaces, however it would not support the idea that the consolidation algorithm proposed to arrange episodes in the hippocampus also works to arrange lower-dimensional representations in other brain regions. Whatever the case, it remains a pressing concern to develop solid theory of the medial temporal lobe, grounded in computational models which explicate the roles and developmental processes of its functional cell types. These models must be able to explain the wide variety of functions of the medial temporal lobe, from spatial navigation to conceptual navigation and episodic memory.

Acknowledgments

I extend so many thanks to Dave Huber for serving as my research advisor and mentor over the past two years and throughout the work culminating in this thesis manuscript. From persuading me to take his graduate level Cognitive Psychology course, to working with me to test multiple neural network models of cognition using simulations, behavioral experimentation, and neuroimaging, Dave has fully engrained in me the importance of utilizing both computational and empirical approaches in the quest to understand the mind and brain. I promise to continue to emphasize this integrative approach in my work moving forward. As many thanks to Rosie Cowell, who like Dave served as a fantastic role model for integrating modeling and experimental approaches in psychology and neuroscience. As my committee member, Rosie provided as much guidance and mentorship as most thesis chairs, and her kind support saved me on multiple occasions from the despair of null results. I look forward to working more closely with Rosie next year as a lab manager and research associate in the Computational Memory and Perception Lab. Many thanks also to David Ross, who was crucial to this project, provided many key insights and contributions, and mentored me in the techniques of cognitive neuroscience all along the way. Finally, I thank my parents Lisa and James, my brother Luke, my girlfriend Emily, and my friends in and out of science, for their love and support of me and my passion for research, even if sometimes I inevitably alienate them with my interests in such convoluted aspects of the neural basis of cognition. I am incredibly lucky to be able to study these problems, and am so excited to continue working towards a deep and nuanced understanding of the brain and mind, and sharing that understanding with others. To all, THANK YOU!

Works Cited

Barry, C., Lever, C., Hayman, R., Hartley, T., Burton, S., O'Keefe, J., … Burgess, N. (2006). The boundary vector cell model of place cell firing and spatial memory. Reviews in the Neurosciences, 17(1–2), 71–97.

Bjerknes, T. L., Moser, E. I., & Moser, M. B. (2014). Representation of geometric borders in the developing rat. Neuron, 82(1), 71–78.

Bonnevie, T., Dunn, B., Fyhn, M., Hafting, T., Derdikman, D., Kubie, J. L., … Moser, M.-B. (2013). Grid cells require excitatory drive from the hippocampus. Nature Neuroscience, 16(3),

Brouwer, G. J., & Heeger, D. J. (2009). Decoding and Reconstructing Color from Responses in Human Visual Cortex. Journal of Neuroscience, 29(44), 13992–14003.

Bussey, T. J., & Saksida, L. M. (2007). Memory, Perception, and the Ventral Visual-Perirhinal-Hippocampal Stream: Thinking Outside of the Boxes. Hippocampus, 17, 898:908.

Constantinescu, A. O., O'Reilly, J. X., & Behrens, T. E. J. (2016). Organizing conceptual knowledge in humans with a grid-like code. Science, 352(6292), 1464–1467.

Derrington, A. M., Krauskopf, J., & Lennie, P. (1984). Chromatic mechanisms in lateral geniculate nucleus of Macaque. The Journal of Physiology, 357, 241–65.

Doeller, C. F., Barry, C., & Burgess, N. (2010). Evidence for grid cells in a human memory network. Nature, 463(7281), 657–661.

Fyhn, M., Molden, S., Witter, M. P., Moser, E. I., & Moser, M. B. (2004). Spatial representation in the entorhinal cortex. Science, 305(5688), 1258–1264.

Hales, T. C. (2006). A proof of the Kepler Conjecture. Annals of Mathematics, 162, 1065-1185.

Hafting, T., Fyhn, M., Molden, S., Moser, M., & Moser, E. I. (2005). Microstructure of a spatial map in the entorhinal cortex. Nature, 436(7052), 801–806.

Hartley, T., Burgess, N., Lever, C., Cacucci, F., & O'Keefe, J. (2000). Modeling place fields in terms of the cortical inputs to the hippocampus. Hippocampus, 10(4), 369–379.

Lafer-Sousa, R., Conway, B. R., & Kanwisher, N. G. (2016). Color-Biased Regions of the Ventral Visual Pathway Lie between Face- and Place-Selective Regions in Humans, as in Macaques. The Journal of Neuroscience, 36(5), 1682–97.

Lever, C., Burton, S., Jeewajee, A., O'Keefe, J., & Burgess, N. (2009). Boundary vector cells in the subiculum of the hippocampal formation. The Journal of Neuroscience : The Official Journal of the Society for Neuroscience, 29(31), 9771–9777.

MacLeod, D. I., & Boynton, R. M. (1979). Chromaticity diagram showing cone excitation by stimuli of equal luminance. Journal of the Optical Society of America.

McClurkin, J. W., & Optican, L. M. (1996). Primate striate and prestriate cortical neurons during discrimination. I. simultaneous temporal encoding of information about color and pattern. Journal of Neurophysiology, 75(1), 481–495.

McClurkin, J. W., Zarbock, J. A., & Optican, L. M. (1996). Primate Striate and Prestriate Cortical Neurons During Discrimination II. Separable Temporal Codes for Color and Pattern.

McNaughton, B. L., Battaglia, F. P., Jensen, O., Moser, E. I., & Moser, M.-B. (2006). Path integration and the neural basis of the "cognitive map." Nat Rev Neurosci, 7(8), 663–678.

Moser, E. I., Kropff, E., & Moser, M.-B. (2008). Place cells, grid cells, and the brain's spatial representation system. Annual Review of Neuroscience, 31, 69–89.

Mumford, J. A., Turner, B. O., Ashby, F. G., & Poldrack, R. A. (2012). Deconvolving BOLD activation in event-related designs for multivoxel pattern classification analyses. NeuroImage, 59(3), 2636–2643.

O'Keefe, J., & Burgess, N. (1996). Geometric determinants of the place fields of hippocampal neurons. Nature.

O'Keefe, J., & Dostrovsky, J. (1971). The hippocampus as a spatial map: Preliminary evidence from unit activity in the freely moving rat. Brain Research, 34, 171–175.

O'Keefe, J., & Nadel, L. (1978). The Hippocampus as a Cognitive Map. Oxford University Press.

Rentzeperis, I., Nikolaev, A. R., Kiper, D. C., & van Leeuwen, C. (2014). Distributed processing of color and form in the visual cortex. Frontiers in Psychology, 5(AUG), 1–14.

Shapley, R., & Hawken, M. J. (2011). Color in the Cortex: Single- and double-opponent cells. Vision Research, 51(7), 701–717.

Solomon, S. G., & Lennie, P. (2007). The machinery of colour vision. *Nature Reviews. Neuroscience*, *8*(4), 276–86.

Solstad, T., Boccara, C. N., Kropff, E., Moser, M.-B., & Moser, E. I. (2008). Representation of geometric borders in the entorhinal cortex. Science, 322(December), 1865–1868.

Solstad, T., Moser, E. I., & Einevoll, G.T. (2006). From Grid Cells to Place Cells: A Mathematical Model. Hippocampus, 17(9), 801–812.